



Multi-scheme chemical ionization inlet (MION) for fast switching of reagent ion chemistry in atmospheric pressure chemical ionization mass spectrometry (CIMS) applications

5 Matti P. Rissanen^{1,2}, Jyri Mikkilä³, Siddharth Iyer⁴, Jani Hakala³

¹Department of Physics and Institute for Atmospheric and Earth System Research, University of Helsinki, Helsinki, Finland

²Aerosol Physics Laboratory, Physics Unit, Faculty of Engineering and Natural Sciences, Tampere University, Tampere, Finland

10 ³Karsa Ltd., A. I. Virtasen aukio 1, 00560 Helsinki, Finland

⁴Department of Chemistry and Institute for Atmospheric and Earth System Research, University of Helsinki, Helsinki, Finland

Correspondence to: Matti P. Rissanen (matti.rissanen@tuni.fi), Jani Hakala (jani.hakala@karsa.fi)

Abstract. A novel chemical ionization inlet (*Multi-scheme chemical IONization inlet*, MION, Karsa Ltd, Helsinki, Finland) capable of fast switching between multiple reagent ion schemes is presented and its performance is demonstrated by measuring several known oxidation products from much studied cyclohexene and α -pinene ozonolysis systems, by applying consecutive bromide (Br^-) and nitrate (NO_3^-) chemical ionization. Experiments were performed in flow tube reactors under atmospheric pressure and room temperature (22°C) utilizing *atmospheric pressure interface time-of-flight mass spectrometer* (API-ToF-MS, Tofwerk Ltd, Thun, Switzerland) as the detector. The application of complementary ion modes in probing the same steady-state reaction mixture enabled a far more complete picture of the detailed autoxidation process; the HO_2 radical and the least oxidized reaction products were retrieved with Br^- ionization, whereas the highest oxidized reaction products were detected in the NO_3^- mode, directly informing on the first steps and on the ultimate end-point of oxidation, respectively. While chemical ionization inlets with multiple reagent ion capabilities have been reported previously, an application in which the charging of the sample occurs at atmospheric pressure with practically no sample pretreatment, and with the potential to switch the reagent ion scheme within a second time-scale, has not been introduced previously. Also, the ability of bromide ionization to detect *highly-oxygenated organic molecules* (HOM) from atmospheric autoxidation reactions has not been demonstrated prior to this investigation.

Keywords: Mass Spectrometry, Chemical ionization, CIMS, CI-API-ToF, HOM, Peroxy radicals, HO_2 and RO_2 , Autoxidation, Atmospheric Acids

1 Introduction

Chemical ionization mass spectrometry (CIMS) is a versatile analysis technique that enables detection of gas-phase molecular constituents at atmospheric pressure and at concentrations as low as 10^5 cm^{-3} (Munson and Field, 1966; Munson, 1977; Eisele and Tanner, 1993; Huey, 2007; de Gouw and Warneke, 2007; Mauldin et al., 2012; Sipilä et al., 2015; Hyttinen et al., 2018; Laskin et al., 2018). With the right selection of reagent ions that either form adducts with the analytes or transfer their electric charge (*e.g.*, with an electron or a proton transfer), CIMS can offer a soft, selective, and extremely sensitive online detection for virtually any gas-phase chemical compounds. In recent years, various CIMS methods have revolutionized the ways we understand atmospheric *volatile organic compound* (VOC) oxidation processes (*see e.g.*, Ehn et al., 2014; Rissanen et al., 2014; Jokinen et al., 2015; Kirkby et al., 2016; Lee et al., 2016; Breitenlechner et al., 2017), especially the routes leading to oxidative molecular growth [*i.e.*, *fast autoxidation* (Crouse et al., 2013; Berndt et al., 2015; Rissanen et al., 2015) and *slow aging* (Donahue et al., 2006; Hallquist et al., 2009)] and subsequent *secondary organic aerosol* (SOA) formation.

In principle, a mass spectrometer is a universal detector with applicability mainly controlled by two factors: (i) volatility, and (ii) ionizability of the analyte (Baeza-Romero et al., 2011; McLafferty, 2011). In practice, the sampled material must be volatilized into the gas-phase and then ionized by a suitable method. In a gas-phase atmospheric application, the problem reduces to the latter, as the analytes are inherently aloft in the surrounding gas media. Unfortunately, the most universal ionization methods, by definition, lack the selectivity needed for separating compounds from complex gas mixtures and information from multiple complementary techniques are generally required to enable chemical speciation (*e.g.*, *isomer separation*), with ambiguity nevertheless quickly increasing with the complexity of the target molecule. The utilization of multiple ionization schemes in CIMS has the potential for detailed chemical speciation of the target compounds by exploiting chemical selectivity, *e.g.*, characterizing amines by ethanol CIMS (Yu and Lee, 2012), peroxy acids by $\text{I}^+\text{H}_2\text{O}^-$ (Iyer et al., 2017), and hydroperoxides by CF_3O^- (Crouse et al., 2006). However, CIMS



55 instruments and their ion sources are expensive and bulky, and consequently, most research laboratories have access to a
precious few. Ideally, a versatile, easily deployable chemical ionization source capable of rapid switching between
multiple reagent ions with varying chemical selectivity would be indispensable in tackling the complexity encountered in
various gas-phase environments.

60 CIMS inlets with multiple reagent ion capabilities have been reported previously (*e.g.*, Jordan et al., 2009; Brophy
and Frammer, 2015), perhaps most commonly in applications concerning *proton transfer reaction mass spectrometry*
(PTRMS). In addition to the usual H_3O^+ reagent ion (Hansel et al., 1995), NO^+ and O_2^+ (Jordan et al., 2009), water clusters
of H_3O^+ (*i.e.*, $(\text{H}_2\text{O})_n\text{H}_3\text{O}^+$) (Breitenlechner et al., 2017), NH_4^+ (Zhang et al., 2018), and a few others [*see* (Blake et al.,
2009) and references therein] have been employed. *Selected ion flow tube* (SIFT) applications have similarly utilized
 H_3O^+ , NO^+ , and O_2^+ ionization schemes augmented further (*in certain applications*) by their fast switching and combined
65 use of simultaneous reagent ions (Smith and Španel, 2005). For similar mass spectrometric detection as in the current
work, Brophy and Farmer (Brophy and Frammer, 2015) have introduced a fast, switchable source for two concomitant ion
mode operation and demonstrated it with the common low-pressure CIMS reagent ions acetate (CH_3COO^-) and iodide (I^-).
Also, other switchable ion sources have been introduced (*e.g.*, Hearn and Smith, 2004; Agarwal et al., 2014; Pan et al.,
2017), but with roughly similar utilization and performance characteristics as the ones presented above. In all these
70 previously reported techniques the sample ionization occurs at reduced pressure, constituting sample pretreatment in
drawing the atmospheric pressure material into the vacuum chambers of the MS and consequently diluting the sample
considerably (*i.e.*, by a factor of about 10 to 10^3). This renders almost any detection method useless in targeting analytes
with very low gas-phase concentrations, such as ambient aerosol precursors *sulfuric acid* (SA) and individual *highly*
oxidized multifunctional compounds (HOM, '*highly oxygenated organic molecules*'), which are present at around 10^5
75 cm^{-3} to 10^7 cm^{-3} (Ehn et al., 2014; Rissanen et al., 2014; Jokinen et al., 2015; Kirkby et al., 2016). Also, dilution through
a small orifice and subsequent turbulent mixing of ions into the sample in the low-pressure CIMS enhances recombination
loss-processes (*e.g.*, *radical-radical combination reactions and wall reactions of reactive and sticky compounds*) causing
depletion and subsequent detection bias. The current design is virtually devoid of these issues as the ionization occurs at
atmospheric pressure by an ion insertion and the sample passes the ion source unperturbed.

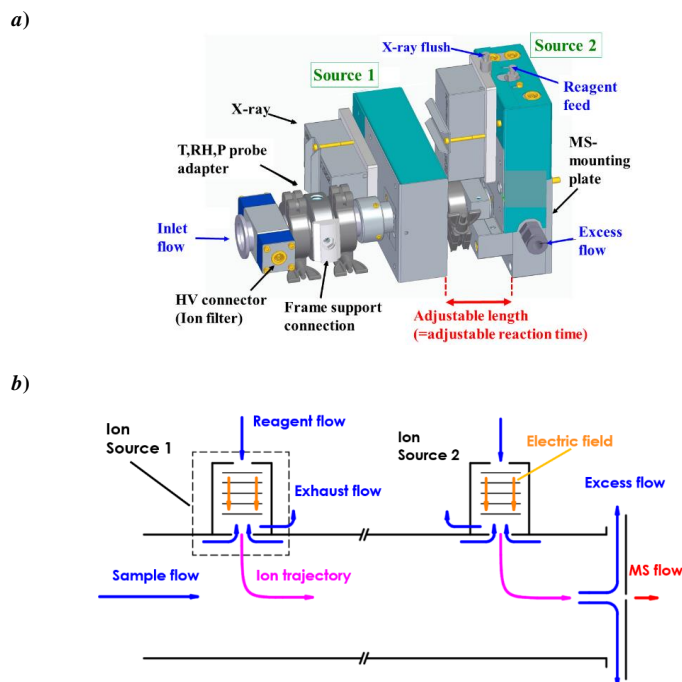
80 While the utilization of multiple reagent ions within a single CIMS apparatus offers significant benefits, to this
date it has not been reported in applications in which the ionization occurs at ambient pressure. Here we introduce a
significant leap in the CIMS methodology by enabling atmospheric pressure sampling and ionization with multiple
consecutive reagent ions in fast repetition, and without any pre-treatment of the sampled gas mixture. When considering
the detection of low-volatile, *in-situ* aerosol precursor compounds such as HOM that lack analytical standards, have a
85 range of individual detection sensitivities (Hytinen et al., 2015; Hytinen et al., 2018), whose transmission and
fragmentation are dependent on the detailed MS settings (Heinritzi et al., 2016; Zapadinsky et al., 2019) and the detection
sensitive to changes in temperature (Frege et al., 2018), it becomes evident that retrieving complementary data depending
on only one instrument calibration factor is extremely valuable. In the newly developed *Multi-scheme chemical*
IONization inlet (MION) described here, the only changing parameter between the ionization stages is the ion specific
90 sensitivity to the target compounds as a function of the ion-molecule reaction time - which does not differ between
applications. We report the characteristics and operation principle of this new inlet and compare its performance against
previously reported CIMS inlets, by coupling it into an *atmospheric pressure time-of-flight mass spectrometer* (APi-ToF-
MS; Junninen et al., 2010) and measuring a multitude of previously reported oxidation products from much studied
cyclohexene and α -pinene ozonolysis systems (*e.g.*, Yokouchi et al. 1985; Hatakeyama et al., 1985; Rissanen et al., 2014;
95 Rissanen et al., 2015). To the best of our knowledge, a current type of an ambient pressure application in which the
reagent ion scheme can be switched *quantitatively* within a second time-scale by simply switching a few voltages, has
not been introduced previously.

100 2 Description of the MION

100 Schematic of the *Multi-scheme chemical IONization inlet*, MION, (Karsa Ltd.) is presented in Figure 1. The inlet consists
of an electrically grounded 24 mm *inner diameter* (*i.d.*) flow tube with multiple coupled ion sources (*simplified two-*
source setup shown in Figure 1). A gas-phase stream of nitrogen or air is enriched with the reagent ion precursor by
feeding it through a saturator (*or the precursor is obtained directly from a gas cylinder*). The resulting reagent flows are
105 then fed into their respective ion sources, where the reagents are ionized by a soft x-ray radiation (*Hamamatsu L12535*).
The reagent ions are then accelerated and focused through 5 mm orifices into the laminar sample flow by electric fields.
Small counterflows are applied through the orifices to prevent the mixing of the electrically neutral reagent precursors
with the sample flow. Besides the ion source orifices, the flow tube design differs only minimally from tubular, making
the flow pattern easy to define, the flow being essentially a flow through a circular pipe. The distance between the
110 downstream ion source and the mass spectrometer pinhole is fixed, but the modular design of the MION allows the
upstream source distance to be chosen to suit the application, with around 50 *milliseconds* (ms) minimum between
ionization stages and longer times achievable by increasing the pipe length between the sources. For the experiments
described in this paper the reaction time for the upstream reagent (*nitrate ion*, NO_3^-) was 300 ms, and for the downstream
reagent (*bromide ion*, Br^-) 30 ms, when the total sample flow was 20 *liters per minute* (lpm).



115



120

Figure 1: The Multi-scheme chemical IONization inlet (MION). *a)* Schematic description of the modular design shown with two concomitant ion sources (SOURCE 1 and 2) with adjustable ion-molecule reaction Time between the two sources, coupled to an ion filter and meteorology sensor. *b)* Illustration of the gas flows and ion paths within the inlet.

125

2.1 Operating the MION

MION is operated by first turning on the counterflows for the ion sources, followed by turning on the sample flow, after which the reagent feed is turned on. The sample flow is controlled by a 50 lpm *mass flow controller* (mfc), and the counterflows and reagent feeds are controlled by 100 *milliliters per minute* (mlpm) mfc's. The flow rates for the reagent feeds and counterflows depend on the compounds used as reagent ion precursors, but generally suitable counterflow (*i.e.*, the counterflow setting subtracted by the reagent feed flow setting) for the ion sources is as little as 25 mlpm. After the flows have been chosen, the high voltage (*c.a.* 2500 V) for the ion accelerator arrays is turned on. Lastly, to guide the reagent ions to the center of the sample flow, the ion deflector voltage (*c.a.* 250 V) for the selected ion source is turned on. Selecting the ion mode (*i.e.*, switching the ionization scheme), is as simple as turning on the deflector voltage for the desired ion source, or turning off (*to 0 V*) both deflectors for ambient ion mode. Turning off both deflectors simultaneously will result in the downstream ion source ionization scheme to apply, as the downstream deflector will deflect most of the ions from the upstream one. While there may be settings where multiple chemical ionization schemes can work simultaneously, the application described in this paper was not designed nor tested for that.

140

2.2 Switching the ion chemistry

The MION design enables rapid, concomitant application of multiple reagent ion chemistries, which selection and combination are mainly dictated by three variables: (*i*) target species to be ionized, (*ii*) characteristics of the reagent ion source compound, and (*iii*) the details of the ion-molecule reaction chemistry [*e.g.*, *adduct formation vs charge transfer* (Hyttinen et al., 2018)]. By considering these issues it is possible to choose a combination of ionization schemes that critically supplement each other, significantly increasing the chemical information obtained from the targets. For example, measuring “a complete” product distribution with an inherently unselective reagent ion (*e.g.*, bicarbonate, HCO_3^-) followed by a step-wise increase in chemical selectivity on further ionization stages [*e.g.*, peroxy acids by $\text{I}^+\text{H}_2\text{O}$ (Iyer et al., 2017) and hydroperoxides by CF_3O^+ (Crouse et al., 2006)]. Similarly, adduct forming reagent ions (*e.g.*, NO_3^-) can

150

3



be augmented with ions strongly participating in further ion-molecule reactions with characteristic reaction and fragmentation patterns. Moreover, the design of the MION is ideally suited for investigating the detailed influence of ion-molecule reaction times (*and thus also ion-molecule reaction kinetics*), enabled by using the same reagent ion precursor feed for multiple ion sources. While in principle any combination of reagent ions is possible in the MION, for this work Br^- and NO_3^- were selected not only due to their differing ionization characteristics but also for their potential to offer complementary insight into the inspected VOC oxidation processes.

The fast switching between the ion modes is illustrated in Figure 2, where the signals obtained for the reagent ions (*i.e.*, Br^- and NO_3^-) and the *total ion current* (TIC) are shown for an experiment where both ionization modes and a natural ion measurement (*labeled APi in Figure 2*) were utilized. The rapid, quantitative ion mode switch is achieved within about a second timeframe with negligible interference from the idle ion mode (*i.e.*, *no lingering background signals from the second reagent ion*).

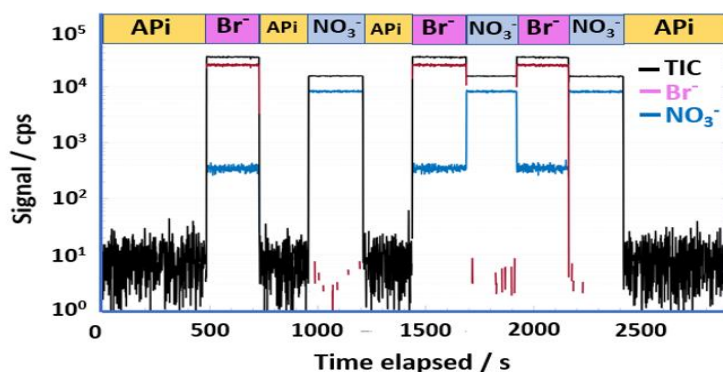


Figure 2 Demonstrating switching between multiple ion chemistries. Abbreviations used: APi = *ambient ion mode*, Br⁻ = *bromide ion mode*, NO₃⁻ = *nitrate ion mode*, TIC = *total ion count*.

3 Characterizing the MION – Sensitivity to gas-phase aerosol precursors

Sensitivity of the MION was inspected in two independent ways: (*i*) by calibrating its response in both ion modes to photochemically produced sulfuric acid (SA, H_2SO_4), and (*ii*) by measuring oxidation products of ozonolysis initiated autoxidation of cyclohexene and α -pinene, especially targeting HOMs (Rissanen et al., 2014; Rissanen et al., 2015). These very low-volatile, *in-situ* atmospheric aerosol precursor compounds are typically present at around 10^5 to 10^7 cm^{-3} concentrations in the ambient gas-phase, and thus an ability to directly detect them will testify the new inlet design's applicability for conducting field measurements. In addition, the SA calibration has been the standard method for estimating nitrate CIMS response to HOM detection (Ehn et al., 2014; Rissanen et al., 2015), which completely lacks any analytical standards, and, the HOM product distributions of these two prototypical endocyclic alkenes are currently the best known.

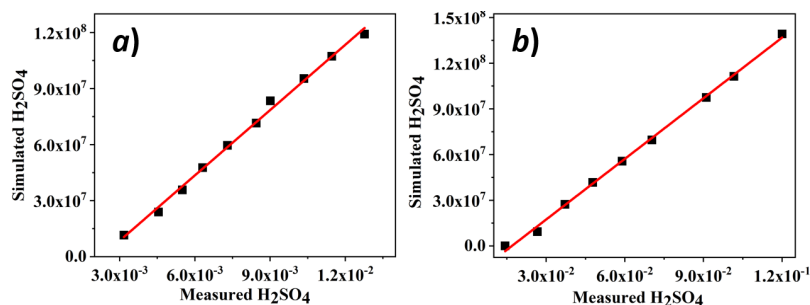
3.1 Sulfuric acid calibration

Figure 3 shows the determined SA calibration plots, in which the measured H_2SO_4 is compared to values deduced by a reaction system simulation of OH initiated SO_2 photo-oxidation (*see the SI for details*). In both ion modes the MION detects gas-phase SA with good linearity of detection and well down to atmospheric concentration levels, with common sunlit daytime values generally ranging between 10^6 to 10^7 cm^{-3} (Eisele and Tanner, 1993; Sipilä et al., 2010). However, the sensitivities between the ion modes had about a factor of 10 difference, perhaps somewhat fortuitously, equaling the difference between the ion-molecule reaction times. The determined calibration factors were $C_{\text{NO}_3^-} = (1.39 \pm 0.03) \times 10^9$ $\text{cm}^{-3} \text{cps}^{-1}$ for the nitrate mode with 300 ms ionization time, and $C_{\text{Br}^-} = (1.32 \pm 0.02) \times 10^{10}$ $\text{cm}^{-3} \text{cps}^{-1}$ for the bromide mode at 30 ms ionization, where the uncertainties refer to the statistical errors of the fits only. The overall uncertainty in the measured H_2SO_4 values obtained with this procedure was previously determined as 33% (Kürten et al., 2012), and the resulting uncertainties in HOM detection have been reported previously as $\pm 50\%$ (Ehn et al., 2014) or a factor of 2 (Berndt et al., 2015).

The obtained $C_{\text{NO}_3^-}$ value compares well with the lower limit values reported previously for the nitrate CIMS employing APi-ToF-MS as the detector, which range roughly from 10^9 to 10^{10} $\text{cm}^{-3} \text{cps}^{-1}$ (*e.g.*, Ehn et al., 2014; Rissanen et al., 2014; Berndt et al., 2015; Jokinen et al., 2015). For the Br^- mode there are no previous values reported for SA detection. However, the HO_2 radical detected well at roughly few ppt concentrations in the flow reactor experiments



195 described next is in accordance with the observations of Albrecht et al. (Albrecht et al., 2018) and Sanchez et al. (Sanchez
et al., 2016).

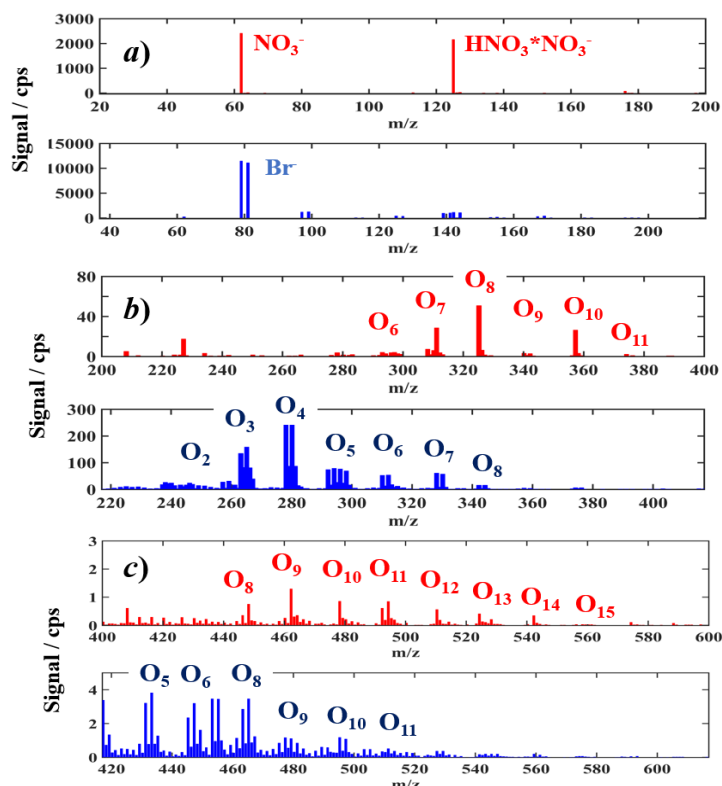


200 **Figure 3** Sulfuric acid (H₂SO₄, SA) calibration plots showing the simulated values against the measured ion signals
determined for a) Br⁻ ion mode, and for b) NO₃⁻ ion mode.

3.2 VOC oxidation products

205 Cyclohexene (C₆H₁₀) and α -pinene (C₁₀H₁₆) ozonolysis initiated autoxidation were investigated to inspect the applicability
of the new inlet design to detect various reaction products with differing oxygen content, and to compare its performance
to previously reported results obtained with other CIMS inlets (e.g., Ehn et al., 2014; Rissanen et al., 2014; Berndt et al.,
2015; Mentel et al., 2015). The experiments were performed in quartz flow tube reactors (2.44 cm i.d. and 80 cm length
or 7.7 cm i.d. and 120 cm length) under atmospheric conditions with an inlet flow of 20 lpm for the MION, resulting in
2 to 10 second reaction times. The hydrocarbon precursor, at around 100 ppb in nitrogen (N₂), was mixed with the bath
210 gas air (N₂ + O₂) and ozone (O₃, c.a. 50 ppb), few centimeters upstream of the flow reactor. The introduction of ozone
into the flow reactor containing the hydrocarbon precursor resulted in apparent instantaneous formation and subsequent
detection of various HOM products, implying that rapid autoxidation of the endocyclic precursors took place, and that
the new inlet design can detect these *in-situ* aerosol precursors present at very low concentrations [i.e., fractions of ppt to
several ppt for individual HOM as reported previously for short reaction time conditions (Jokinen et al., 2015; Berndt et
215 al., 2016)]. More details of the experimental setup and conditions can be found in the SI chapter S2.

Typical spectra obtained with the MION during an α -pinene ozonolysis experiment in both ion modes are shown
in Figure 4 (for cyclohexene spectra see the SI); the bromide spectra have been shifted 17 mass units to illustrate common
compositions on top of each other in the spectra, and the mass peak ranges have been divided into the reagent ion,
monomer and dimer mass ranges (see Figure 4 and Figure S1 in the SI). Inspecting the obtained spectra, it becomes
220 immediately evident that only the bromide ionization retrieves few of the least-oxidized reaction products (but to a large
extent also the further oxidized compounds), whereas the extremely selective NO₃⁻ ionization is a lot more sensitive to
the highest oxidized species. However, in the present work, a 10 times longer ion-molecule reaction time was used for
the NO₃⁻ mode, and thus the sensitivity to the higher oxidized products could be augmented, at least partly, by this longer
reaction time which generally leads to increased sensitivity for the strongest bound reagent*product adducts, and thus to
225 the highest oxidized reaction products (Hytinen et al., 2015; Hytinen et al., 2018). Nevertheless, the charging mechanism
between these reagent ions differ; in nitrate ionization the analyte and HNO₃ compete for NO₃⁻ whereas, in bromide
ionization, Br⁻ directly forms adducts with the analyte, i.e., ligand switching reaction instead of direct adduct formation
(Hytinen et al. 2015; Hytinen et al. 2018), leading to inherently less selective ionization by Br⁻. Additionally, bromide
ionization results in significantly more organic ion products devoid of the reagent ion, implying that other ion-molecule
230 reactions are also involved in Br⁻ ionization [e.g., deprotonation (Hansel et al., 2015; Breitenlechner et al., 2017) or
dehydroxylation (Mielke et al., 2012; Iyer et al., 2017)] than simply adduct formation (see the SI for further details). In
contrast, NO₃⁻ was only observed to deprotonate a few dicarboxylic acids and SA reported in previous publications (Eisele
et al., 1993; Rissanen et al., 2014). The organic ions were always minor in comparison to the most prominent product
peaks.



235

Figure 4 Example MION spectra obtained from α -pinene ozonolysis experiments shown with a common product mass axis for both ion modes, *i.e.*, the Br^- spectrum (blue) is displaced by 17 Th (=difference between reagent ion Br^- and NO_3^- masses) to overlap the same composition products horizontally. **a)** Illustrates the reagent ion spectra, **b)** the monomer range (*i.e.*, oxidation products which have the same number or less carbon atoms), and **c)** the dimer range (*i.e.*, oxidation products with about two times the carbon number of α -pinene), respectively. The amount of oxygen atoms in detected products have also been illustrated.

240

The concomitant application of NO_3^- and Br^- ionization is enabled by their comparable adduct binding strengths (Hytinen et al., 2018), which means that both product-adducts are seen at around similar efficiency with the same mass spectrometer settings, and that strong adduct fragmentation would be seen in both ion modes if present. With very different product*adduct binding strengths, the least-bound adducts could easily be lost due to fragmentation in the API section of the MS. However, if the charging mechanism between the two reagent modes differ (*e.g.*, one forms adducts and the other transfers charge), then they are likely applicable together, and are largely unaffected by the mass spectrometer settings.

245

The fast switching of observed peroxy radical (RO_2 and HO_2) reagent*product adducts is illustrated in Figure 5, where the ion signals obtained for the reagent ions and several α -pinene oxidation products are shown for an experiment in which the O_3 concentration was varied. The rapid ion mode change is completed within about one second timeframe and is seen, for example, in the time traces measured for the prominent, highly-oxidized peroxy radical formed by autoxidation, $\text{C}_{10}\text{H}_{15}\text{O}_{10}$ (Rissanen et al., 2015), which was detected well in both ion modes. Here, switching of the ion mode only shifts the mass of the product peak in the spectrum, with associated shift in signal intensity due to differences in the absolute detection sensitivities and total ion counts between the ion modes. In contrast, the HO_2 radical and the primary ozonolysis derived peroxy radical, $\text{C}_{10}\text{H}_{15}\text{O}_4$, are detected only in the Br^- mode and thus disappear from the spectrum (*i.e.*, from the time trace shown) when nitrate mode is utilized. Similarly, few of the most oxidized reaction products were prominent only in the NO_3^- spectra (Figure 4).

250

255

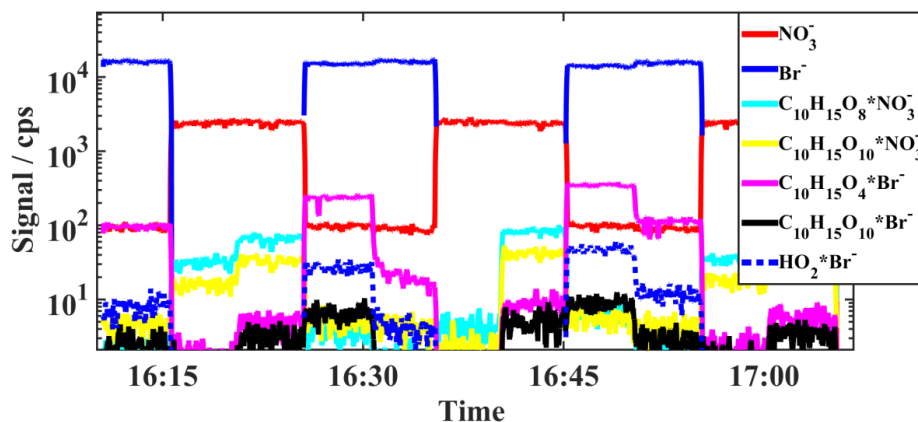


Figure 5 Time traces measured for the reagent ions and selected α -pinene oxidation derived peroxy radicals illustrating the fast switching between reagent ion modes; the prominent highly oxidized RO₂ (C₁₀H₁₅O₁₀) is retrieved by both ion modes, whereas, primary peroxy radicals HO₂ and C₁₀H₁₅O₄ were solely detected with Br⁻ ionization. The changes in the product signal levels are due to different VOC and ozone loads in the flow reactor experiments.

4.1 Comparison to previously reported cyclohexene and α -pinene HOM product distributions

The cyclohexene ozonolysis HOM product distribution reported previously in Rissanen et al. (Rissanen et al., 2014), Berndt et al. (Berndt et al., 2015) and Mentel et al. (Mentel et al., 2015) is well recorded by the NO₃⁻ ion mode of the MION, and even extends to the somewhat less oxidized reaction products. This is likely due to the different ion injection process in the current inlet design which could potentially concomitantly decrease the sensitivity for the highest oxidized compounds (Hytinen et al., 2015). However, the observed sensitivity to the highest oxidized species is similar within the measurement uncertainties to our previous works (*e.g.*, Rissanen et al., 2014; Rissanen et al., 2015) and all the previously reported HOM by NO₃⁻ ionization are detected with the MION setup too.

In the bromide mode, also the least oxidized reaction products down to 2 O-atoms were recorded, which amply illustrates the benefit from the multiple ion operation. To the best of our knowledge, this is the first-time bromide ionization has been used to detect gas-phase cyclohexene and α -pinene ozonolysis products and thus a direct comparison to previous results is not possible. Nevertheless, the Br⁻ ionization retrieves even earlier reaction products in cyclohexene oxidation than those reported with the acetate (CH₃COO⁻) (Berndt et al., 2015; Hytinen et al., 2017) and iodide (I⁻) (Mielke et al., 2012; Iyer et al., 2017) reagent ions. For α -pinene, in addition to the HOMs reported previously by NO₃⁻ ionization (*e.g.*, Ehn et al., 2014; Rissanen et al., 2015), bromide picks up several products with compositions matching the well-known, abundant, early generation oxidation products (*e.g.*, pinic acid C₉H₁₄O₄) (Ma et al., 2007) but which could also result from isomeric product compounds detected at the same exact mass. Additionally, ozonolysis of endocyclic alkenes produces a range of smaller carboxylic and peroxy acids as primary and secondary reaction products (Johnson and Marston, 2008), some of which were also detected in the current experiments with high sensitivity (*e.g.*, based on the current alkene + O₃ reaction rates, these products should be present at around maximum 1 ppb concentration with the long reaction time and high VOC loading experiments). Formic acid (HCOOH) and acetic acid (CH₃COOH) were detected in the experiments, together with peaks having matching compositions to higher carboxylic acids, but which do not have unambiguous molecular compositions for definite mass specific identification. In addition, the strong acids nitric acid (HNO₃) and sulfuric acid (H₂SO₄) were also detected in the bromide mode, the latter used in calibration, and the former being a by-product of unrelated NO_x experiments performed with the same inlet system.

4.2 Comparison to previously reported CIMS applications using multiple reagent ions

The MION inlet represents a significant improvement in measuring analytes at atmospheric pressure by employing multiple complementary ion chemistries. As mentioned above, to our knowledge, this is the only application in which the ionization occurs under ambient conditions and is completely devoid of any sample pre-treatment. Perhaps closest to the current application is the two-ion-mode setup introduced by Brophy and Farmer (Brophy and Farmer, 2015), in which the ionization scheme is likewise changed by a simple ion optics voltage switching, but which operates under reduced pressures (*roughly at 0.1 Atm*), inherently lowering the sensitivity to the electrically neutral target compounds. Crucially, the MION is not limited to two-ion-mode operation described in the present paper and, due to its modular design, can



300 accommodate as many reagent ions as feasible, only limited by space, utilizable ion-molecule reaction times and other physicochemical constraints set by the reagent precursors.

The recently developed PTRMS instruments (Breitenlechner et al., 2014; Krechmer et al., 2018) can, in principle, rival the multi-ion operation due to their wide detection range for different oxidized states, and their applicability for direct ambient pressure sampling. However, in practice, the product analysis is tedious due to the inherently low selectivity of the common H⁺ transfer reagents, resulting in vast number of overlapping compounds. Yet again, the ionization in PTRMS instruments occurs at low pressures (*commonly around 1 mbar*), resulting in sample dilution discussed above.

5. Conclusions

310 Atmospheric pressure chemical ionization mass spectrometry utilizing multiple reagent ion chemistries is a powerful analysis method for probing various gas-phase processes. The new type of inlet design introduced here enables selective inspection of gas-phase product distributions, allowed by rapid switching of chemical selectivity via specific reagent ion chemistries. This principle was demonstrated by detecting various previously reported oxidation products of cyclohexene and α -pinene applying Br⁺ and NO₃⁺ ionization schemes in parallel. The sensitivity of the MION was observed to rival the previously reported CIMS inlets in detecting HOMs and sulfuric acid, exemplifying its applicability for field deployments. While the current setup was optimized for two-ion-mode operation, the modular construction of the MION enables it to, in principle, operate with multiple, unlimited ionization stages in fast repetition and without any instrument or sample pre-treatment, the ion mode being changed by a simple switching of a few low voltage settings.

320 Acknowledgements

MPR is grateful for the support from the Academy of Finland (Grant number 299574).

Supporting Information

325 The Supporting Information material includes sections S1-S6: S1 Abstract – description of the supporting material, S2 Experimental setup and conditions, S3 Ion signal to concentration conversion, S4 Calibration measurement, S5 Product distributions – specific reaction products, S6 Organic ion peaks devoid of the reagent ion. Supporting Figures S1-S3; example MION spectra.

References

- 330 1. Agarwal, B., Méndez, R. G., Lanza, M., Sulzer, P., Märk, T. D., Thomas, N., and Mayhew, C. A.: Sensitivity and Selectivity of Switchable Reagent Ion Soft Chemical Ionization Mass Spectrometry for the Detection of Picric Acid, *J. Phys. Chem. A*, 118, 8229-8236, 2014.
2. Albrecht, S. R., Novelli, A., Hofzumahaus, A., Kang, S., Baker, Y., Mentel, T., Wahner, A., and Fuchs, H.: Measurements of hydroperoxy radicals (HO₂) at atmospheric concentrations using bromide chemical ionization mass spectrometry, *Atmos. Meas. Tech.*, 12, 891-902, 2019.
- 335 3. Baeza-Romero, M. T., Blitz, M. A., Goddard, A., and Seakins, P. W.: Time-of-flight mass spectrometry for time-resolved measurements: Some developments and applications, *Int J. Chem. Kin.*, 44, 532-545, 2011.
4. Berndt, T., Richters, S., Kaethner, R., Voigtländer, J., Stratmann, F., Sipilä, M., Kulmala, M., and Herrmann, H.: Gas-Phase Ozonolysis of Cycloalkenes: Formation of Highly Oxidized RO₂ Radicals and Their Reactions with NO, NO₂, SO₂, and Other RO₂ Radicals, *J. Phys. Chem. A*, 119, 10336-10348, 2015.
- 340 5. Blake, R. S., Monks, P. S., and Ellis, A. M.: Proton-Transfer Reaction Mass Spectrometry, *Chem. Rev.*, 109, 861-896, 2009.
6. Breitenlechner, M., Fischer, L., Hainer, M., Heinritzi, M., Curtius, J., and Hansel, A.: PTR3: An Instrument for Studying the Lifecycle of Reactive Organic Carbon in the Atmosphere, *Anal. Chem.*, 89, 5824-5831, 2017.
- 345 7. Brophy, P. and Farmer, D. K.: A switchable reagent ion high resolution time-of-flight chemical ionization mass spectrometer for real-time measurement of gas phase oxidized species: characterization from the 2013 southern oxidant and aerosol study, *Atmos. Meas. Tech.*, 8, 2945-2959, 2015.
8. Crouse, J. D., McKinney, K. A., Kwan, A. J., and Wennberg, P. O.: Measurement of Gas-Phase Hydroperoxides by Chemical Ionization Mass Spectrometry, *Anal. Chem.*, 78, 6726-6732, 2006.
- 350 9. Crouse, J. D., Nielsen, L. B., Jørgensen, S., Kjaergaard, H. G., and Wennberg, P. O.: Autoxidation of Organic Compounds in the Atmosphere, *J. Phys. Chem. Lett.*, 4, 3513-3520, 2013.
10. Donahue, N. M., Robinson, A. L., Stanier, C. O., and Pandis, S. N.: Coupled Partitioning, Dilution, and Chemical Aging of Semivolatile Organics, *Environ. Sci. Technol.*, 40, 2635-2643, 2006.
- 355 11. Ehn, M., Thornton, J. A., Kleist, E., Sipilä, M., Junninen, H., Pullinen, I., Springer, M., Rubach, F., Tillmann, R., Lee, B., Lopez-Hilfiker, F., Andres, S., Acir, I.-H., Rissanen, M., Jokinen, T., Schobesberger, S., Kangasluoma, J., Kontkanen, J., Nieminen, T., Kurtén, T., Nielsen, L. B., Jørgensen, S., Kjaergaard, H. G., Canagaratna, M., Dal Maso, M., Berndt, T., Petäjä, T., Wahner, A., Kerminen, V.-M., Kulmala, M., Worsnop,



- D. R., Wildt, J., and Mentel, T. F.: A large source of low-volatility secondary organic aerosol, *Nature*, 506, 476-479, 2014.
- 360 12. Eisele, F. L. and Tanner, D. J.: Measurement of the gas phase concentration of H₂SO₄ and methane sulfonic acid and estimates of H₂SO₄ production and loss in the atmosphere, *J. Geophys. Res. Atmospheres*, 98, 9001-9010, 1993.
- 365 13. Frege, C., Ortega, I. K., Rissanen, M. P., Praplan, A. P., Steiner, G., Heinritzi, M., Ahonen, L., Amorim, A., Bernhammer, A.-K., Bianchi, F., Brilke, S., Breitenlechner, M., Dada, L., Dias, A., Duplissy, J., Ehrhart, S., El-Haddad, I., Fischer, L., Fuchs, C., Garmash, O., Gonin, M., Hansel, A., Hoyle, C. R., Jokinen, T., Junninen, H., Kirkby, J., Kürten, A., Lehtipalo, K., Leiminger, M., Mauldin, R. L., Molteni, U., Nichman, L., Petäjä, T., Sarnela, N., Schobesberger, S., Simon, M., Sipilä, M., Stolzenburg, D., Tomé, A., Vogel, A. L., Wagner, A. C., Wagner, R., Xiao, M., Yan, C., Ye, P., Curtius, J., Donahue, N. M., Flagan, R. C., Kulmala, M., Worsnop, D. R., Winkler, P. M., Dommen, J., and Baltensperger, U.: Influence of temperature on the molecular composition of ions and charged clusters during pure biogenic nucleation, *Atmos. Chem. Phys.*, 18, 65-79, 2018.
- 370 14. de Gouw, J. and Warneke, C.: Measurements of volatile organic compounds in the earth's atmosphere using proton-transfer-reaction mass spectrometry, *Mass. Spectrom. Rev.*, 26, 223-257, 2007.
- 375 15. Hallquist, M., Wenger, J. C., Baltensperger, U., Rudich, Y., Simpson, D., Claeys, M., Dommen, J., Donahue, N. M., George, C., Goldstein, A. H., Hamilton, J. F., Herrmann, H., Hoffmann, T., Iinuma, Y., Jang, M., Jenkin, M. E., Jimenez, J. L., Kiendler-Scharr, A., Maenhaut, W., McFiggans, G., Mentel, Th. F., Monod, A., Prévôt, A. S. H., Seinfeld, J. H., Surratt, J. D., Szmigielski, R., and Wildt, J.: The formation, properties and impact of secondary organic aerosol: current and emerging issues, *Atmos. Chem. Phys.*, 9, 5155-5236, 2009.
- 380 16. Hansel, A., Jordan, A., Holzinger, R., Prazeller, P., Vogel, W., and Lindinger, W.: Proton transfer reaction mass spectrometry: on-line trace gas analysis at the ppb level, *Int. J. Mass Spectrom. Ion Process.*, 149, 609-619, 1995.
- 385 17. Hatakeyama, S., Tanonaka, T., Weng, J.-H., Bandow, H., Takagi, H., and Akimoto, H.: Ozone-Cyclohexene Reaction in Air: Quantitative Analysis of Particulate Products and the Reaction Mechanism, *Environ. Sci. Technol.*, 19, 935-942, 1985.
- 390 18. Hearn, J. D. and Smith, G. D.: A Chemical Ionization Mass Spectrometry Method for the Online Analysis of Organic Aerosols, *Anal. Chem.*, 76, 2820-2826, 2004.
- 395 19. Heinritzi, M., Simon, M., Steiner, G., Wagner, A. C., Kürten, A., Hansel, A., and Curtius, J.: Characterization of the mass-dependent transmission efficiency of a CIMS, *Atmos. Meas. Tech.*, 9, 1449-1460, 2016.
- 400 20. Huey, L. G.: Measurement of trace atmospheric species by chemical ionization mass spectrometry: Speciation of reactive nitrogen and future directions, *Mass Spectrom. Rev.*, 26, 166-184, 2007.
- 405 21. Hyttinen, N., Kupiainen-Määttä, O., Rissanen, M. P., Muuronen, M., Ehn, M., and Kurtén, T.: Modeling the Detection of Highly Oxidized Cyclohexene Ozonolysis Products Using Nitrate-Based Chemical Ionization, *J. Phys. Chem. A*, 119, 6339-6345, 2015.
- 410 22. Hyttinen, N., Rissanen, M. P., and Kurtén, T.: Computational Comparison of Acetate and Nitrate Chemical Ionization of Highly Oxidized Cyclohexene Ozonolysis Intermediates and Products, *J. Phys. Chem. A*, 121, 2172-2179, 2017.
- 415 23. Hyttinen, N., Otkjær, R. V., Iyer, S., Kjaergaard, H. G., Rissanen, M. P., Wennberg, P. O., and Kurteň, T.: Computational Comparison of Different Reagent Ions in the Chemical Ionization of Oxidized Multifunctional Compounds, *J. Phys. Chem. A*, 122, 269-279, 2018.
24. Iyer, S., He, X., Hyttinen, N., Kurtén, T., and Rissanen, M. P.: Computational and Experimental Investigation of the Detection of HO₂ Radical and the Products of Its Reaction with Cyclohexene Ozonolysis Derived RO₂ Radicals by an Iodide-Based Chemical Ionization Mass Spectrometer, *J. Phys. Chem. A*, 121, 6778-6789, 2017.
25. Johnson, D., and Marston, G.: The gas-phase ozonolysis of unsaturated volatile organic compounds in the troposphere, *Chem. Soc. Rev.*, 37, 699-716, 2008.
- 405 26. Jokinen, T., Berndt, T., Makkonen, R., Kerminen, V.-M., Junninen, H., Paasonen, P., Stratmann, F., Herrmann, H., Guenther, A. B., Worsnop, D. R., Kulmala, M., Ehn, M., and Sipilä, M.: Production of extremely low volatile organic compounds from biogenic emissions: Measured yields and atmospheric implications, *Proc. Natl. Acad. Sci.*, 112, 7123-7128, 2015.
27. Jordan, A., Haidacher, S., Hanel, G., Hartungen, E., Herbig, J., Märk, L., Schottkowsky, R., Seehauser, H., Sulzer, P., and Märk, T. D.: An online ultra-high sensitivity Proton-transfer-reaction mass-spectrometer combined with switchable reagent ion capability (PTR + SRI - MS), *Int. J. Mass Spectrom.*, 286, 32-38, 2009.
- 410 28. Junninen, H., Ehn, M., Petäjä, T., Luosujärvi, L., Kotiaho, T., Kostianinen, R., Rohner, U., Gonin, M., Fuhrer, K., Kulmala, M., and Worsnop, D. R.: A high-resolution mass spectrometer to measure atmospheric ion composition, *Atmos. Meas. Tech.*, 3, 1039-1053, 2010
- 415 29. Kirkby, J., Duplissy, J., Sengupta, K., Frege, C., Gordon, H., Williamson, C., Heinritzi, M., Simon, M., Yan, C., Almeida, J., Tröstl, J., Nieminen, T., Ortega, I. K., Wagner, R., Adamov, A., Amorim, A., Bernhammer, A.-K., Bianchi, F., Breitenlechner, M., Brilke, S., Chen, X., Craven, J., Dias, A., Ehrhart, S., Flagan, R. C., Franchin, A., Fuchs, C., Guida, R., Hakala, J., Hoyle, C. R., Jokinen, T., Junninen, H., Kangasluoma, J., Kim, J., Krapf,



- 420 M., Kürten, A., Laaksonen, A., Lehtipalo, K., Makhmutov, V., Mathot, S., Molteni, U., Onnela, A., Peräkylä, O., Piel, F., Petäjä, T., Praplan, A. P., Pringle, K., Rap, A., Richards, N. A. D., Riipinen, I., Rissanen, M. P., Rondo, L., Sarnela, N., Schobesberger, S., Scott, C. E., Seinfeld, J. H., Sipilä, M., Steiner, G., Stozhkov, Y., Stratmann, F., Tomé, A., Virtanen, A., Vogel, A. L., Wagner, A. C., Wagner, P. E., Weingartner, E., Wimmer, D., Winkler, P. M., Ye, P., Zhang, X., Hansel, A., Dommen, J., Donahue, N. M., Worsnop, D. R., Baltensperger, U., Kulmala, M., Carslaw, K. S., and Curtius, J.: Ion-induced nucleation of pure biogenic particles, *Nature*, 533, 521-526, 2016.
- 425 30. Krechmer, J., Lopez-Hilfiker, F., Koss, A., Hutterli, M., Stoermer, C., Deming, B., Kimmel, J., Warneke, C., Holzinger, R., Jayne, J., Worsnop, D., Fuhrer, K., Gonin, M., and de Gouw, J.: Evaluation of a New Reagent-Ion Source and Focusing Ion-Molecule Reactor for Use in Proton-Transfer-Reaction Mass Spectrometry, *Anal. Chem.*, 2018, 90, 12011-12018.
- 430 31. Kürten, A., Rondo, L., Ehrhart, S., and Curtius, J.: Calibration of a Chemical Ionization Mass Spectrometer for the Measurement of Gaseous Sulfuric Acid, *J. Phys. Chem. A*, 116, 6375-6386, 2012.
32. Laskin, J., Laskin, A., and Nizkorodov, S. A.: Mass Spectrometry Analysis in Atmospheric Chemistry, *Anal. Chem.*, 90, 166-189, 2018.
- 435 33. Lee, B. H., Mohr, C., Lopez-Hilfiker, F. D., Lutz, A., Hallquist, M., Lee, L., Romer, P., Cohen, R. C., Iyer, S., Kurtén, T., Hu, W., Day, D. A., Campuzano-Joste, P., Jimenez, J. L., Xu, L., Ng, N. L., Guo, H., Weber, R. J., Wild, R. J., Brown, S. S., Koss, A., de Gouw, J., Olson, K., Goldstein, A. H., Seco, R., Kim, S., McAvey, K., Shepson, P. B., Starn, T., Baumann, K., Edgerton, E. S., Liu, J., Shilling, J. E., Miller, D. O., Brune, W., Schobesberger, S., D'Ambro, E. L., and Thornton, J. A.: Highly functionalized organic nitrates in the southeast United States: Contribution to secondary organic aerosol and reactive nitrogen budgets, *Proc. Natl. Acad. Sci.*, 113, 1516-1521, 2016.
- 440 34. Ma, Y., Willcox, T. R.; Russell, A. T., and Marston, G.: Pinic and pinonic acid formation in the reaction of ozone with α -pinene, *Chem. Comm.*, 1328-1330, 2007.
35. Mauldin III, R. L., Berndt, T., Sipilä, M., Paasonen, P., Petäjä, T., Kim, S., Kurtén, T., Stratmann, F., Kerminen, V.-M., and Kulmala, M.: A new atmospherically relevant oxidant of sulphur dioxide, *Nature*, 488, 193-196, 2012.
- 445 36. McLafferty, F. D.: A Century of Progress in Molecular Mass Spectrometry, *Annu. Rev. Anal. Chem.*, 4, 1-22, 2011.
37. Mentel, T. F., Springer, M., Ehn, M., Kleist, E., Pullinen, I., Pullinen, Kurtén, T., Rissanen, M., Wahner, A., and Wildt, J.: Formation of highly oxidized multifunctional compounds: autoxidation of peroxy radicals formed in the ozonolysis of alkenes – deduced from structure–product relationships, *Atmos. Chem. Phys.*, 15, 2791-2851, 2015.
- 450 38. Mielke, L. H. and Osthoff, H. D.: On quantitative measurements of peroxy-carboxylic nitric anhydride mixing ratios by thermal dissociation chemical ionization mass spectrometry, *Int. J. Mass Spectrom.*, 310, 1-9, 2012.
39. Munson, B.: Chemical Ionization Mass Spectrometry, *Anal. Chem.*, 49, 772A-778A, 1977.
40. Munson, M. S. B., Field, F. H.: Chemical Ionization Mass Spectrometry I: General Introduction, *J. Am. Chem. Soc.*, 88, 2621-2630, 1966.
- 455 41. Pan, Y., Zhang, Q., Zhou, W., Zou, X., Wang, H., Huang, C., Shen, C., and Chu, Y.: Detection of Ketones by a Novel Technology: Dipolar Proton Transfer Reaction Mass Spectrometry (DP-PTR-MS), *J. Am. Soc. Mass Spectrom.*, 28, 873-879, 2017.
42. Rissanen, M. P., Kurtén, T., Sipilä, M., Thornton, J. A., Kangasluoma, J., Sarnela, N., Junninen, H., Jørgensen, S., Schallhart, S., Kajos, M. K., Taipale, R., Springer, M., Mentel, T. F., Ruuskanen, T., Petäjä, T., Worsnop, D. R., Kjaergaard, H. G., and Ehn, M.: The formation of highly oxidized multifunctional products in the ozonolysis of cyclohexene, *J. Am. Chem. Soc.*, 136, 15596-15606, 2014.
- 460 43. Rissanen, M. P., Kurtén, T., Sipilä, M., Thornton, J. A., Kausiala, O., Garmash, O., Kjaergaard, H. G., Petäjä, T., Worsnop, D. R., Ehn, M., and Kulmala, M.: Effects of Chemical Complexity on the Autoxidation Mechanisms of Endocyclic Alkene Ozonolysis Products: From Methylcyclohexenes toward Understanding α -Pinene, *J. Phys. Chem. A*, 119, 4633-4650, 2015.
- 465 44. Sanchez, J., Tanner, D. J., Chen, D., Huey L. G., and N. L. Ng: A new technique for the direct detection of HO₂ radicals using bromide chemical ionization mass spectrometry (Br-CIMS): initial characterization, *Atmos. Meas. Tech.*, 9, 3851-3861, 2016.
- 470 45. Sipilä, M., Sarnela, N., Jokinen, T., Junninen, H., Hakala, J., Rissanen, M. P., Praplan, A., Simon, M., Kürten, A., Bianchi, F., Dommen, J., Curtius, J., Petäjä, T., and Worsnop, D. R.: Bisulfate – cluster based atmospheric pressure chemical ionization mass spectrometer for high-sensitivity (< 100 ppqV) detection of atmospheric dimethyl amine: proof-of-concept and first ambient data from boreal forest, *Atmos. Meas. Tech.*, 8, 4001-4011, 2015.
- 475 46. Sipilä, M., Berndt, T., Petäjä, T., Brus, D., Vanhanen, J., Stratmann, F., Patokoski, J., Mauldin, R. L. 3rd, Hyvärinen, A. P., Lihavainen, H., and Kulmala, M.: The role of sulfuric acid in atmospheric nucleation, *Science*, 327, 1243-1246, 2010.



47. Smith, D. and Španel, P.: Selected ion flow tube mass spectrometry (SIFT-MS) for on-line trace gas analysis, *Mass Spectrom. Rev.*, 24, 661-700, 2005.
- 480 48. Yokouchi, Y. and Ambe Y.: Aerosols formed from the chemical reaction of monoterpenes and ozone, *Atmos. Environ.*, 19, 1271-1276, 1985.
49. Yu, H. and Lee, S-H.: Chemical ionisation mass spectrometry for the measurement of atmospheric amines, *Environ. Chem.*, 9, 190-201, 2012.
50. Zapadinsky, E. Passananti, M., Myllys, N., Kurtén, T., and Vehkamäki H.: Modeling on Fragmentation of
485 Clusters inside a Mass Spectrometer, *J. Phys. Chem. A.*, 123, 611-624, 2019.
51. Zhang, Q., Zou, X., Liang, Q., Wang, H., Huang, C., Shen, C., and Chu, Y.: Ammonia-Assisted Proton Transfer Reaction Mass Spectrometry for Detecting Triacetone Triperoxide (TATP) Explosive, *J. Am. Soc. Mass Spectrom.*, 30, 501-508, 2019.